THE ASTROPHYSICAL JOURNAL, Vol. 157, August 1969

EARLY SUPERNOVA LUMINOSITY

STIRLING A. COLGATE AND CHESTER MCKEE
New Mexico Institute of Mining and Technology, Socorro
Received October 17, 1968; revised January 20, 1969

ABSTRACT

The diffusion of radiant energy from spherical expanding matter has been analytically and numerically calculated for masses and velocities of model supernova outbursts. The agreement with observation is satisfactory. The production of a large mass fraction of the radioactive isotope ^{56}Ni, which has been predicted from calculations of supernova nucleosynthesis, appears to be critical for the formation of the observed light curves. The radioactive energy from 0.25 $M_\odot$ of ^{56}Ni by the decay process $^{56}\text{Ni} \rightarrow {}^{56}\text{Co}$ (6^d.01, Ec, 1.72 MeV of γ-rays per decay) supplies the radiant energy, 10^{49} ergs, during the "diffusive release" phase (5–20 days) of expansion near maximum. The subsequent decay process, $^{56}\text{Co} \rightarrow {}^{56}\text{Fe}$ (77 days, Ec, 3.59 MeV of γ-rays), in conjunction with progressive γ-ray transparency of the expanding matter, gives rise to the long-time exponential light decay of 35–65 days. The velocity distribution with the best fit (Type I supernovae) gives $\langle V^2 \rangle = (1.6 \times 10^9 \text{ cm sec}^{-1})^2$. For a pure thermonuclear supernova requiring a minimum of 1.4 $M_\odot$ of ^{12}C, the implied kinetic energy is 3 times the maximum available from ^{12}C burning, and 6 times that available from the model calculated by Hansen. This implies the possibility that some supernovae originated from neutron stars.

I. INTRODUCTION

The early optical emission from supernova has been both quantitatively and qualitatively a mystery. The rise time of 1 week has been interpreted by Poveda (1964) as indicating ejection of 0.01 $M_\odot$, while line emission and Doppler shifts indicate ejection of 0.1–10 $M_\odot$ (Minkowski 1964, 1968). The spectrum is totally unexplained (Zwicky 1965), and the ejection velocity of 10^8 cm sec^{-1} observed for old remnants (Poveda and Woltjer 1968) is at variance with that of 2×10^9 cm sec^{-1}, interpreted for the newest remnant, Tycho's star (Minkowski 1964). Theory has been no more helpful, as Schatzman (1965) admits. The supernova calculations of Colgate and White (1966) depended on the release of the relatively large binding energy ($\sim 10^{53}$ ergs) of the dynamically formed neutron star, a fraction of which (10–30 percent) appears as kinetic energy of ejected matter. However, the predicted optical energy was small, and an attempt to explain this by assuming the presence of a large (2 $M_\odot$) amount of radioactive (allowed β-decay) matter was even then inadequate to explain the observed luminosity.

The problem is that the heat energy of the expanding matter is converted to kinetic energy by adiabatic expansion long before it is liberated as radiant heat. The later the liberation of heat energy, the smaller the subsequent adiabatic expansion before release. Cameron and Arnett (1967) attempted an explanation based on late burning of deuterium, but the neutron release and subsequent heavy-element production were inconsistent with r-process abundances. Instead, and as a consequence, we have been stimulated to perform the present calculation by the results of nucleosynthesis calculations; namely, James Truran recommended that we take a look at the consequences of silicon-burning (Truran, Arnett, and Cameron 1967). This process leads to the α-particle isotope ^{56}Ni as the predominant end product of thermonuclear processes. (^{56}Ni is the minimum in the packing-fraction curve for α-particle nuclei.) The decay scheme of ^{56}Ni (Lederer *et al.* 1967), shown in Figure 1, is $^{56}\text{Ni}(6^d.01) \rightarrow {}^{56}\text{Co}(77^d) \rightarrow {}^{56}\text{Fe}$. The release of the relatively large energy (1.72 MeV per ^{56}Ni decay) during the optimum and critical time period of $\sim$6 days, in which diffusive release of the radiant heat energy occurs, produces the optical luminosity. As a consequence, we have taken the material-expansion curves from previous hydrodynamic calculations and appended onto them

the β-decay energy of the expected 0.25 $M_\odot$ of ^{56}Ni and ^{56}Co. From these we have reproduced with a numerical diffusion program the observed time and luminosity behavior of early light curves of supernovae. We have started this work with an analytic solution using one set of simplifying assumptions. This solution illuminated the important features of the problem, as well as satisfying the necessity for obtaining a suitable test problem to simulate and test the extreme conditions required of the numerical program. A phenomenological approach to the problem of supernova light curves is developed first.

II. VELOCITY OF THE EJECTED MATTER

A supernova is presumed to be the explosion of a self-gravitating sphere of gas—a star. Furthermore, the star is commonly presumed to be approaching the end of nucleosynthesis. As a consequence, the matter density must be large (10^5–10^{10} g cm^{-3}) in order that the gravitational field can contain in equilibrium the temperature associated

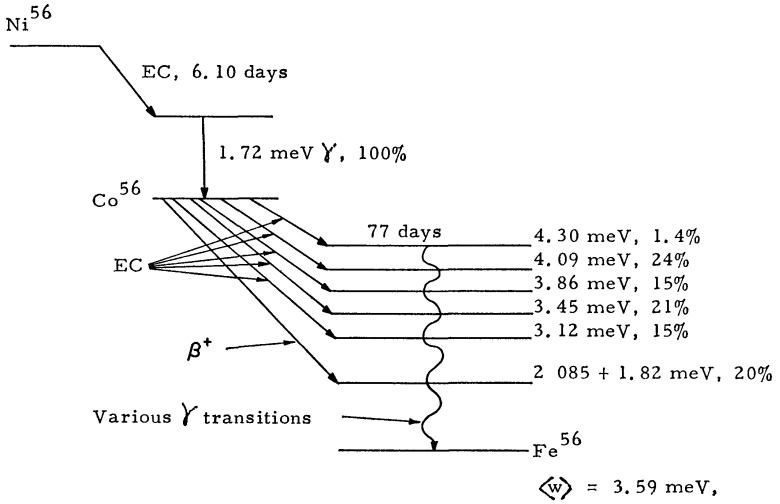

FIG. 1.—^{56}Ni → ^{56}Co → ^{56}Fe decay scheme (*Nuclear Data Sheets*)

with the final stages of nuclear burning. Regardless whether the explosion is thermonuclear, triggered by collapse (Burbidge *et al.* 1957; Rakavy and Shaviv 1967; Fraley 1968; Hansen and Wheeler 1968; Arnett 1968*a*,*b*), or whether the binding energy of the resulting neutron star is transported to the mantle by neutrinos (Colgate and White 1966; Arnett 1967; Schwartz 1967), the explosion is nearly the same; namely, roughly 1 solar mass is ejected with a mean velocity corresponding to the gravitational binding energy just before explosion and with a velocity distribution depending on the relative location of the mass fraction in question. The simplest velocity distribution is that of a uniform spherical expansion (density independent of radius), $V = V_1 r/r_0$, where r_0 is the outer boundary, $V_1 t$; or

$$V = V_1(1 - F)^{1/3} \tag{1}$$

where F is the external mass fraction,

$$F = \frac{1}{M_{ej}} \int_r^\infty 4\pi r^2 \rho dr \,, \tag{2}$$

where M_{ej} is the ejected mass. Figure 2 shows where the velocity distribution of equation (1) is matched at the mass fraction, $F = 0.42$, to a velocity distribution (eq.[3]) of the external layers resulting from the speedup of the shock wave progressing in the density

gradient of the outer layers of the star. The hydrodynamic results of Colgate and White for supernovae of 1.5 $M_\odot$ and 10 $M_\odot$ are included for comparison. The external velocity distribution is

$$V = V_2 F^{-1/4} . \quad (3)$$

For the case of a supernova produced by the formation of a neutron star, the constants $V_1 = 3 \times 10^9$ cm sec^{-1} and $V_2 = 2 \times 10^9$ cm sec^{-1} result in an average kinetic energy of 3.7×10^{18} ergs g^{-1}. This energy is roughly 4.2 times that achievable from helium burning and 7.4 times that possible from carbon burning, if gravitational binding is excluded. The curves for the velocity distribution when both V_1 and V_2 are reduced by $\frac{1}{2}$ and $\frac{1}{4}$ are shown, as well as the velocity distribution resulting from the ^{12}C thermonuclear hydrodynamic calculation of Hansen and Wheeler (1968). As would be expected, the form of the velocity distribution is approximately independent of the mechanism of explosion; the velocity scale depends only upon the total energy.

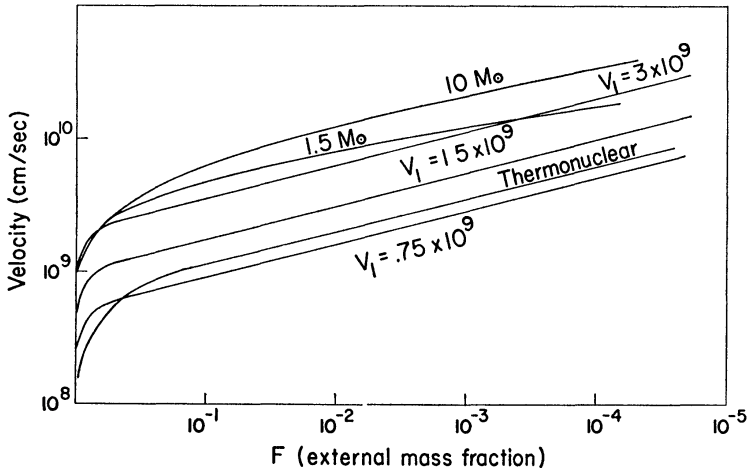

FIG. 2.—Velocity versus mass fraction for a series of analytic curves corresponding to equations (1) and (3). For comparison, the velocity distributions of the neutron-star supernova of Colgate and White (1966) and of the thermonuclear supernova of Hansen and Wheeler (1968) are added.

III. DIFFUSIVE RELEASE OF RADIANT ENERGY

It is assumed that the velocity distributions of equations (1) and (3) are first created by heating the gas by thermonuclear reactions, neutrino deposition, or a shock wave, and that subsequent adiabatic expansion converts the heat into kinetic energy of ejection. It is further assumed that the initial heat source has decayed to insignificance long before the time (several days) that expansion has proceeded to the point of bolometric maximum. The residual energy associated with each mass element is that remaining after adiabatic expansion from the initial heating, as well as that introduced by other energy sources such as radioactivity or collision with the interstellar medium. This latter luminosity due to collisional heating has been discussed in connection with the far greater luminosity of quasi-stellar sources (Colgate and Cameron 1963; Colgate 1967) and in connection with Seyfert galaxies (Colgate 1968), but it is unlikely to be the principal cause of the average supernova luminosity. The minimum circumstellar density required to give the observed peak luminosity is 10^4 H atoms cm^{-3} at $r = 10^{17}$ cm, which is typical of planetary nebulae. Then the luminosity becomes $L \leq 4\pi r^2 \rho_0 V^{3/2}$ ergs sec^{-1}. However, the rise time of the light emission cannot be much less than $\frac{1}{3}rV - 1 \geq 6$ months, compared with the observed 1 week. Although some supernovae might fit this model, the requirement that such a nebula be conditional for all super-

novae appears too restrictive. Instead, we will investigate internal sources of energy such as radioactivity.

The energy densities associated with the velocity distributions of equations (1) and (3) are large enough that a major fraction of the internal energy is in the form of radiation rather than particle energy. As a consequence, the diffusive flow of radiation proceeds as a separate "gas," and the specific heat of the matter becomes insignificant. Under these conditions, a diffusive wave of radiation will penetrate a plane-parallel distance ∂ in a time t according to the error-function solution,

$$\partial = (Dt)^{1/2}, \tag{4}$$

where the diffusion coefficient $D = \frac{1}{3}c/K\rho$ (where K = opacity, ρ = density). During the expansion of the matter, each mass element will follow an adiabatic law modified by any energy sources until a diffusive wave penetrates from the surface to the mass element in question. This diffusive wave will "release" the internal energy presumably at peak luminosity when the diffusive wave has penetrated to a depth $\partial \simeq \frac{1}{3}r_0$ corresponding to one-half the ejected mass. Equating the diffusion time obtained from equation (4) with $\partial = \frac{1}{3}r_0$ to the expansion time r_0/V_1 gives

$$r_0/\lambda = 3c/V_1, \tag{5}$$

where λ = the radiation mean free path = $(K\rho)^{-1}$. In other words, the star will be relatively thick ($3c/V_1 \simeq 30$ mean free paths) at the time of the diffusive release of the bulk of the internal energy. If we let $\rho = 3M/(4\pi r_0^3)$ in equation (5) and neglect the density gradient, we obtain

$$t = \left(\frac{KM}{4\pi c V_1}\right)^{1/2} \text{sec}. \tag{6}$$

If $M = 1\ M_\odot$, $K = 0.2$ g cm^{-2} (Compton), and $V_1 = 3 \times 10^9$ cm sec^{-1}, then $t = 6 \times 10^5$ sec (7 days), and the matter will have expanded from $\rho = 10^{9\pm3}$ g cm^{-3} to $\rho \simeq 2.5 \times 10^{-13}$ g cm^{-3}. The large expansion ratio of $4 \times 10^{21\pm3}$ reduces the largest possible initial internal energy, U_0, of 4×10^{18} ergs g^{-1} to $2.6 \times 10^{11\pm1}$ ergs g^{-1} ($U = U_0\ \rho^{-1/3}$), if an adiabatic expansion is assumed with $\gamma = \frac{4}{3}$ for a radiation-dominated gas. The total internal energy that can be radiated is then only $UM_\odot = 5 \times 10^{44\pm1}$ ergs, which is $10^{-3.3\pm1}$ of that estimated for the average supernova, 10^{49} ergs, of either type (Minkowski 1964). The fact that part of the adiabat may proceed with $\gamma = \frac{5}{3}$ only further reduces the available radiant energy. Two possibilities remain: Either a source of radioactive energy exists in the expanding matter which gives heat energy late in time, or the shock-heated matter undergoes less expansion, owing to an initial expanded stellar structure. This latter possibility was investigated by Colgate and White, and the assumption of a red-giant structure ($r \simeq 1.5 \times 10^{13}$ cm) as calculated by Hofmeister, Kippenhahn, and Weigert (1964) and the relatively large shock-energy input of 10^{52} ergs resulted in a bolometric luminosity one-sixtieth of that observed. As a consequence, one is forced to consider either a more expanded initial structure ($r \simeq 10^{14}$ cm) or late sources of radioactive energy.

IV. ANALYTICAL SOLUTION WITH ALLOWED β-DECAY

a) Method

The most general radioactive energy source is one composed of an ensemble of β-decays. (The α-particle decay of heavy nuclei or spontaneous-fission nuclei are presumed too low in abundance, despite their high decay energies, to contribute significantly to the radioactive energy.) It was further assumed that the ensemble of β-decay nuclei would be on the neutron-rich side of the stability curve analogous to fission-product nuclei, but of lower isotopic mass. Such a statistical ensemble of radioactive decays leads to the well-known rate of decay proportional to $t^{-1.2}$, as observed for fission products. (An elementary derivation is given in Colgate and White 1966.)

The rate of β-decay energy release then becomes $S = S_0\, t^{-1.4}$, and the constant, $S_0 = 5 \times 10^{16}$ ergs g^{-1} sec^{-1}, was chosen as if two allowed β-decays occurred in series per fifty nucleons.

Finally, the velocity trajectory of each mass fraction is presumed to remain constant after the initial expansion; the total β-decay energy is small compared with the ejection kinetic energy, and the velocity distribution of equation (3) was assumed as an adequate approximation for the whole star. Since the initial radius is small compared with the radii of interest, the radius of the expanding matter becomes

$$r = V_2 t F^{-a}, \tag{7}$$

where the Lagrange coordinate, F, is given by equation (2), and a is of the order $\frac{1}{4}$. Then, if one equates $\partial F/\partial r$ from equations (2) and (7), the density becomes

$$\rho = \rho_0 \frac{F^{3a+1}}{t^3}, \tag{8}$$

where $\rho_0 = M/(4\pi a\, V_2{}^3)$.

The energy equation in spherical geometry, including diffusive transport, an energy source, and adiabatic expansion with $\gamma = \frac{4}{3}$, is

$$\frac{du}{dt} - \tfrac{4}{3}\frac{u}{\rho}\frac{d\rho}{dt} = \frac{\rho}{r^2}\frac{\partial}{\partial r}\left(r^2 D \frac{\partial u}{\partial r}\right) + \rho S_0, \tag{9}$$

where u is the specific energy density, the diffusion coefficient $D = \frac{1}{3}c/\kappa\rho$, and S_0 is an energy source or sink.

Transforming to Lagrangian coordinates by equations (7) and (8), we obtain the diffusion equation

$$\frac{\partial u}{\partial t} + \frac{4u}{t} = D' F^{3a+1}\frac{\partial}{\partial F}\left[F^{-4a}\frac{\partial u}{\partial F}\right] + \rho_0 S_0 F^{3a+1} t^{\beta_0 - 1}, \tag{10}$$

where $D' = 4\pi c V_2/3aK\rho$ and the β-decay source is $S = S_0 t^{\beta_0+2}$ and β_0 is presumably -3.4. The terms in equation (10) are respectively the net change of energy following a volume element, the adiabatic work, the net balance in diffusive transport, the energy generated due to β-decay.

Use of the method of similarity transformation (Morgan 1952) obtains the transformation

$$u = \rho_0 S_0 \sigma^{2(3a+1)/(a+1)} t^{\nu} G(z); \quad z = \frac{F^{a+1}}{2\sigma^2 t^2}; \quad \sigma = \frac{a+1}{2}\sqrt{D'};$$
$$\nu = \frac{2(3a+1)}{a+1} + \beta_0, \tag{11}$$

and the invariant solution,

$$\begin{aligned} G(z) = {} & AM\left(-\frac{5a+3}{a+1} - \frac{\beta_0}{2}, -\frac{3a}{a+1}; -z\right) + Bz^{(4a+1)/(a+1)} \\ & \times M\left(-\frac{a+2}{a+1} - \frac{\beta_0}{2}, \frac{5a+2}{a+1}; -z\right) \\ & - 2^{2a/(a+1)} \sum_{n=0}^{\infty} \frac{(-1)^n [(2a+3)/(a+1) + \frac{1}{2}\beta_0]_n\, z^{n+(4a+2)/(a+1)}}{n!\,[n+1/(a+1)][(4a+2)/(a+1)]_{n+1}} \\ & \times M\left(-\frac{a+2}{a+1} - \frac{\beta_0}{2}, n + \frac{5a+3}{a+1}; -z\right), \end{aligned} \tag{12}$$

where the solution is obtained by the method of Laplace transforms (Erdelyi *et al.* 1954), and where $M(a, b; z)$ is the Kummer function (Jahnke, Emde, and Losch 1960) and G(z) satisfies the ordinary differential equation,

$$zG'' + \left(-\frac{3a}{a+1} + z\right)G' - \left(\frac{5a+3}{a+1} + \frac{\beta_0}{2}\right)G = -2^{2a/(a+1)}z^{(3a+1)/(a+1)} . \quad (13)$$

To determine the proper boundary conditions to impose, we observe that, in the region of large optical depth,

$$G(z) = B'z^{(5a+3)/(a+1)+\beta_0/2} + \frac{2^{2a/(a+1)}z^{(3a+1)/(a+1)}}{2 + \frac{1}{2}\beta_0} \quad (14)$$

satisfies equation (10) if the diffusion term is zero.

Then, if $t > 0$ and if we assume no energy input other than $S = S_0\, t^{\beta_0+2}$, we can impose the following boundary conditions:

$$\begin{aligned} &\text{i)}\ u(0,t) = 0 \text{ implies } G(0) = 0 ; \\ &\text{ii)}\ u(F,t) = \frac{\rho_0 S_0 F^{3a+1}}{\beta_0 + 4} t^{\beta_0} \text{ as } F \to 1 \text{ implies } G(z) = \frac{2^{2a/(a+1)}z^{(3a+1)/(a+1)}}{2 + \frac{1}{2}\beta_0} \text{ for } z \gg 1 . \end{aligned} \quad (15)$$

Under these boundary conditions the solution is most easily found by using the Runge-Kutta technique to integrate equation (13) numerically. The numerical solution was started with $z = 10^{-4}$ near the outer boundary of the star by using the analytic solutions (12) with $A = 0$, as required by condition (15i), and $B = 12$. As the inner boundary is approached, one evaluates B' in equation (14). If one chooses a value of B, one can estimate graphically and obtain $B \approx 4.2$ as the value which satisfies the boundary condition (15ii). A check performed with $B = 4.19725$ resulted in a value for B' of $\sim 10^{-6}$, the more accurate value being obtained by subtracting out the undesired solution.

If, in addition to the β-decay source, we consider the energy input due to the shock wave produced in the gravitational-collapse model, we can obtain a solution by noting that the density distribution before the shocked layers expand is $\rho = \rho_i F^{-\lambda}$, where $\lambda \simeq 1$. This approximates the polytropic ($n = 3$) distribution where $\lambda = \frac{4}{3}$, but is modified by the small redistribution occurring in the outer layers during the initial collapse phase. In addition, the internal energy of the fluid immediately behind the shock front is roughly one-half the kinetic energy imparted to the fluid by the shock.

These considerations enable us to solve for the adiabatic behavior of the shock-deposited energy; namely,

$$U_s = U_0 \frac{F^{2a+(4-\lambda)/3}}{t^4} , \quad (16)$$

with

$$U_0 = \frac{\rho_0 V_2^2}{8}\left(\frac{\rho_0}{\rho_i}\right)^{1/3} .$$

If we use equation (16) as the boundary conditions in place of condition (15ii) as $F \to 1$ and the second function in equation (12) as the solution, we note that it satisfies the homogeneous part of equation (10) and the boundary conditions (15i) and (16) if we choose

$$\frac{\beta}{2} = \frac{4-\lambda}{3(a+1)} - 3 .$$

This yields

$$U_s = ct^{-2(\lambda+2)/3(a+1)}z^{(4a+1)/(a+1)}M\left(\frac{6a+\lambda-1}{3(a+1)}, \frac{5a+2}{a+1}; -z\right), \quad (17)$$

with

$$c = U_0(2\sigma^2)^{2a/(a+1)+(4-\lambda)/3(a+1)} \frac{\Gamma[(3a+1)/(a+1) + \frac{1}{3}(4-\lambda)/(a+1)]}{\Gamma[(5a+2)/(a+1)]},$$

as the solution for the shock-deposited energy.

The final solution is then the computer solution plus equation (17). We then obtain the luminosity from the relation,

$$L = -4\pi r^2 \frac{c}{3K\rho} \frac{\partial u}{\partial r}, \tag{18}$$

while the surface is defined by

$$F_s = \left(\frac{4a+2}{3a\rho_0 V_2 K}\right)^{1/(2a+1)} t^{2/(2a+1)} \tag{19}$$

which is obtained by evaluating the integral,

$$\int_r^\infty K\rho dr = 2/3 . \tag{20}$$

b) Results

Figures 3 and 4 show the energy density for 10 $M\odot$ and 2 $M\odot$ obtained from the analytic solution as a function of mass fraction and time. The mass fractions smaller than 10^{-4} correspond to relativistic velocities, so the solution is nonphysical for $F \leq 10^{-4}$. The energy density early in time is determined by the shock deposition. Later in time, as adiabatic expansion takes place, the β-decay adds a larger fraction of the residual energy density. The energy density is diffusively released from the mass fractions marked by the solid line $z = 0.6$ in Figures 3 and 4. This region of diffusive release occurs inside the surface (*dashed line*) when the surface velocity is less than c, the limiting velocity for a diffusion wave. The peak luminosity occurs when the diffusive-release condition approaches the center of the star, $F = 1$, at 20 and 7 days, respectively.

Figure 5 shows the luminosity, surface radius, surface velocity, and surface temperature as a function of time for both the 2 $M\odot$ and 10 $M\odot$ cases. Even the extreme and unrealistic case of 10 $M\odot$ of β-radioactive material shows a peak luminosity one-third of that observed. If the expansion velocity were reduced, the luminosity would be further decreased. One is forced to conclude that another energy source exists whose decay is slower than the allowed β-spectrum. (Although a "statistical" initial distribution of neutron-rich nuclei with allowed β-spectra was used as the energy source, $S = S_0 t^{-1}$ [4], at any given time t the energy production is predominantly determined by nuclei with decay constant t^{-1}; hence the generalization of excluding the allowed β-spectrum of neutron-rich neuclei.)

V. COMPUTATIONAL MODEL

The numerical diffusion hydrodynamics program written by Richard White is given in the Appendix. The test of the ability of the numerical program to reproduce the analytical solution is also shown in Figure 5, where the curve is analytic and the points are computed. The close agreement gives confidence in the ability of the computational program to calculate the more general problem.

a) Velocity Distribution

The velocity distribution of a 1.5 $M\odot$ supernova with a presumed 50 percent ejected mass (0.75 $M\odot$) was chosen as typical of a Type I supernova. As discussed following equations (1) and (3), the inner 0.42 mass fraction expands uniformly, and the outer 0.58 mass fraction follows the law, $V = V_2 F^{-1/4}$. Figure 2 shows the distribution used compared with the original explosion calculation of Colgate and White. The reduction

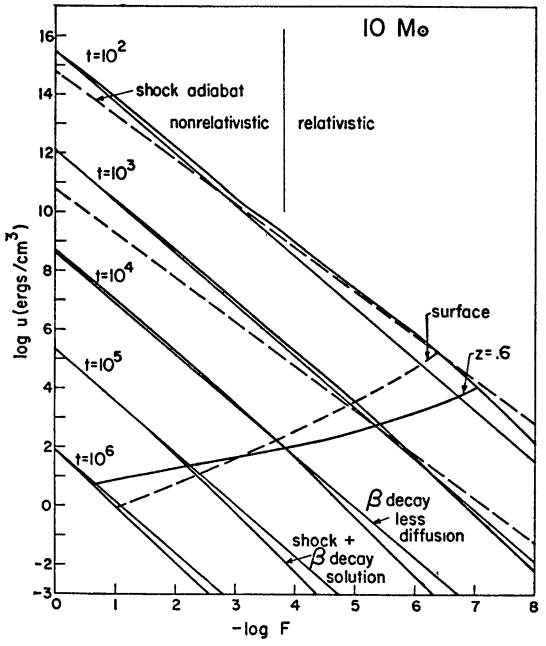

FIG. 3

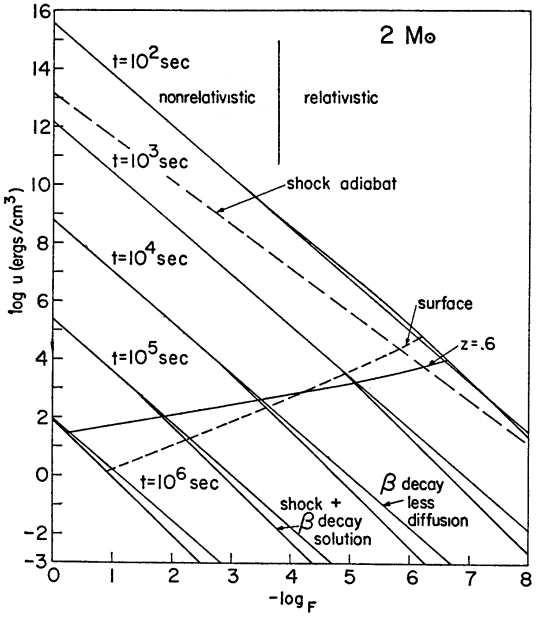

FIG. 4

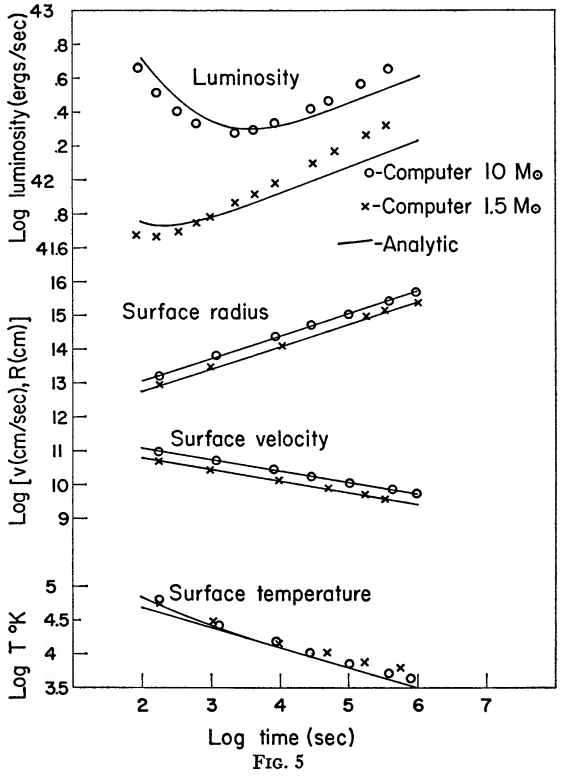

FIG. 5

FIG. 3.—Energy density of supernova ejecta 10 $M\odot$ as a function of mass fraction and time for the analytic solution.

FIG. 4.—Energy density of supernova ejecta 2 $M\odot$ as a function of mass fraction and time for the analytic solution.

FIG. 5.—Comparison of the analytic solution of 2 $M\odot$ and 10 $M\odot$ supernova luminosity versus time with the computational program.

in velocities by a factor of 2 for each distribution was done empirically in an attempt to correlate the resulting light curve with that observed. The same velocity distributions were used for the 10 $M_\odot$ calculations. The quantity $V_1 = 3$, 1.5, and 0.75×10^9 cm sec^{-1}, and $V_2 = 2$, 1, and 0.5×10^9 cm sec^{-1}.

b) Energy Source from the β-Decay $^{56}\mathrm{Ni} \rightarrow {}^{56}\mathrm{Co}$

The results of nucleosynthesis calculations of silicon burning by Bodansky, Clayton, and Fowler (1968*a*,*b*) simplified and clarified the earlier papers of Fowler and Hoyle (1964), Truran, Cameron, and Gilbert (1966), and Truran, Arnett, and Cameron (1967) on the abundances to be expected, and it now appears likely that silicon-burning shells in supernovae are responsible for most of the nucleosynthesis in the range of atomic weight $28 \leq A \leq 57$. The most striking feature of this work is the prediction of the element abundances that is in good agreement with the observed abundances. In particular, the mass peak of ^{56}Fe stands out a factor of 10 above the surrounding isotopes, each of which is reproduced from the calculations with surprisingly good accuracy. The unique feature of the ^{56}Fe peak for the present work is that its origin depends on the formation of the most tightly bound α-particle nucleus ^{56}Ni, which subsequently decays to ^{56}Co and then to ^{56}Fe according to the decay scheme shown in Figure 1. Although adjacent nuclei are also formed that are radioactive, their observed cosmic abundance ($\lesssim$10 percent ^{56}Fe) would indicate that they contribute no more than 10–20 percent to the total β-decay energy of the ^{56}Ni chain. Although we will neglect these other radioactive nuclei in this treatment of the light emission by supernovae, they are by no means unimportant for the possible detection of supernova remnants by the γ-rays resulting from such decays. Indeed, Clayton, Colgate, and Fishman (1969) predict that supernovae out to several megaparsecs should be observable by balloon-borne detectors and that the time behavior of the rising portion of these curves should give a unique determination of the velocity-distribution constants, V_1 and V_2, in equations (1) and (3).

The results of silicon-burning calculations that give the best fit to observed relative abundances predict roughly one-third ^{56}Ni formation and two-thirds ^{28}Si, other nuclei making up a small fraction of the total. Considerations of nucleosynthesis conditions occurring in the strong-shock limit for $V_1 = 3 \times 10^9$ cm sec^{-1} and $V_2 = 2 \times 10^9$ cm sec^{-1} would indicate (from calculations of Truran [1967]) almost 100 percent ^{56}Ni synthesis, in which case the observed abundance of silicon would have to emerge from other less violent events. As a first estimate, the ejected matter was chosen to be one-third ^{56}Ni and two-thirds ^{28}Si. In the case of the 1.5 $M_\odot$ supernova with 0.75 $M_\odot$ ejected, this corresponds to 0.25 $M_\odot$ of ^{56}Ni, which is almost twice that chosen by Clayton, Colgate, and Fishman (0.14 $M_\odot$) as being consistent with galactic abundances and supernova frequency. The resulting light curves, on the other hand, show a bolometric luminosity about equal to that observed, so the first calculations of γ-ray detectability have been performed with what is most likely one-half the mass of ^{56}Ni required.

The decay scheme in Figure 1 indicates that only the 1.72-MeV γ-ray of ^{56}Ni will be deposited as heat, the remaining 0.5 MeV escaping as the electron-capture neutrino. During the "thick" phase of the expansion ($\rho r \gg K_\gamma^{-1}$, $t \leq 10$ days) the γ-rays as well as the positrons from ^{56}Co will be deposited, giving a deposited energy of 3.59 MeV per decay. The remainder will be lost as neutrino emission.

If the decay of ^{56}Ni is given by $N_1 = N_0\, e^{-\lambda_1 t}$, then the number of ^{56}Co, N_2, with decay constant λ_2, is

$$N_2 = \frac{N_0 \lambda_1}{\lambda_2 - \lambda_1} \left(e^{-\lambda_1 t} - e^{-\lambda_2 t}\right), \tag{21}$$

and the energy rate from ^{56}Ni and ^{56}Co becomes

$$S_1 = N_0\lambda_1\epsilon_1 e^{-\lambda_1 t}\,;$$
$$S_2 = \lambda_2 N_{2\epsilon_2} e^{-\lambda_2 t}, \tag{22}$$

whose sum for the decay constants of ^{56}Ni and ^{56}Co, if one-third ^{56}Ni per gram is chosen, is

$$S_0 = 1.15 \times 10^{10} e^{-\lambda_1 t} + 0.252 \times 10^{10} e^{-\lambda_2 t} \text{ ergs g}^{-1} \text{ sec}^{-1}\,. \tag{23}$$

The case of 0.75 $M\odot$ ejected gives a peak energy rate of 2×10^{43} ergs sec^{-1}, which is twice the desired luminosity.

VI. OPACITY

The expected temperature of the matter during the time of interest, 10^3–10^6 sec, in the region of diffusive release ($z \simeq 0.6$), can be estimated from the analytic solution to be $5 \times 10^{3°} \leq T \leq 5 \times 10^{4°}$ K, and densities can be estimated to be $10^{-11} \leq \rho \leq 10^{-15}$ g cm^{-3}. This is just the region of temperature where line opacities may become important. For this reason, a computer run was requested of the program for opacity calculations of Cox and Stewart (1965) for the elements Fe, Cu, He, and H in the above density and temperature range. These are displayed in Figures 6–9 and demonstrate the unique properties of iron. The number of lines in the iron spectrum is so large (500–1000) that, even at the low densities in question the lines contribute significantly ($\times 5$) to the total opacity at $T \simeq 10^{4°}$ K. Since this is approximately the surface temperature, the question arises whether a mixture of all other elements might have the same effect of line "blocking" and give rise to an opacity significantly larger than their individual sum. The final result indicates that the heat flow or total luminosity is determined by the diffusive release of the internal energy from the "bulk" of the mass at considerably higher temperature ($\times 5$) and density ($\times 10$) than the surface. The surface condition, as in any star, adjusts to this total luminosity. However, since we did not know this beforehand, we had to test the significance of this possibility, and so two separate opacities were used. One was iron, increased by the ratio 56/37 which corresponds to a mean molecular weight of 37 (i.e., to one-third ^{56}Ni + two-thirds ^{28}Si), and the other was copper, again with a representative molecular weight of 37. Presumably a mean molecular weight of 37 is the best estimate of the result of silicon burning. The opacity of the inner region, the bulk of the mass, is determined at these low densities entirely by the number of free electrons and hence almost solely by the mean molecular weight. This, in turn, will determine the total luminosity, so the assumption of $\langle\mu\rangle = 37$ is an upper limit to the molecular weight and results in a *lower* limit to the number of free electrons and hence opacity. Consequently the calculated luminosities are upper limits, and any addition of light elements will increase the opacity and will broaden and lower the light curves.

The initial calculations comparing Fe and Cu opacities (Fig. 10) were performed by inadvertently using an erroneous heat-source term—the $^{56}\text{Co} \rightarrow {}^{56}\text{Fe}$ decay (S_2) multiplied by 10, which increases the total energy input late in time during maximum by a factor of 3.2. The calculated luminosity covers a range of 10^4, overlapping and large compared with this factor of 3.2, and over this entire range the two opacities give the same result. Thus, fortunately, the resulting light curves are not sensitive to the additional line opacity of iron, since this is purely a surface effect and does not determine the heat flow in the interior. The line opacity of iron did lead to a calculational instability and a large investment in computer time, so it was not repeated. The effect of the line opacity is to hold back the heat flow; however, the line opacity has the odd property of decreasing with increasing temperature (Fig. 6), so that the heat held back tends to "burn out" the lines, allowing the radiation to escape and cooling and closing the

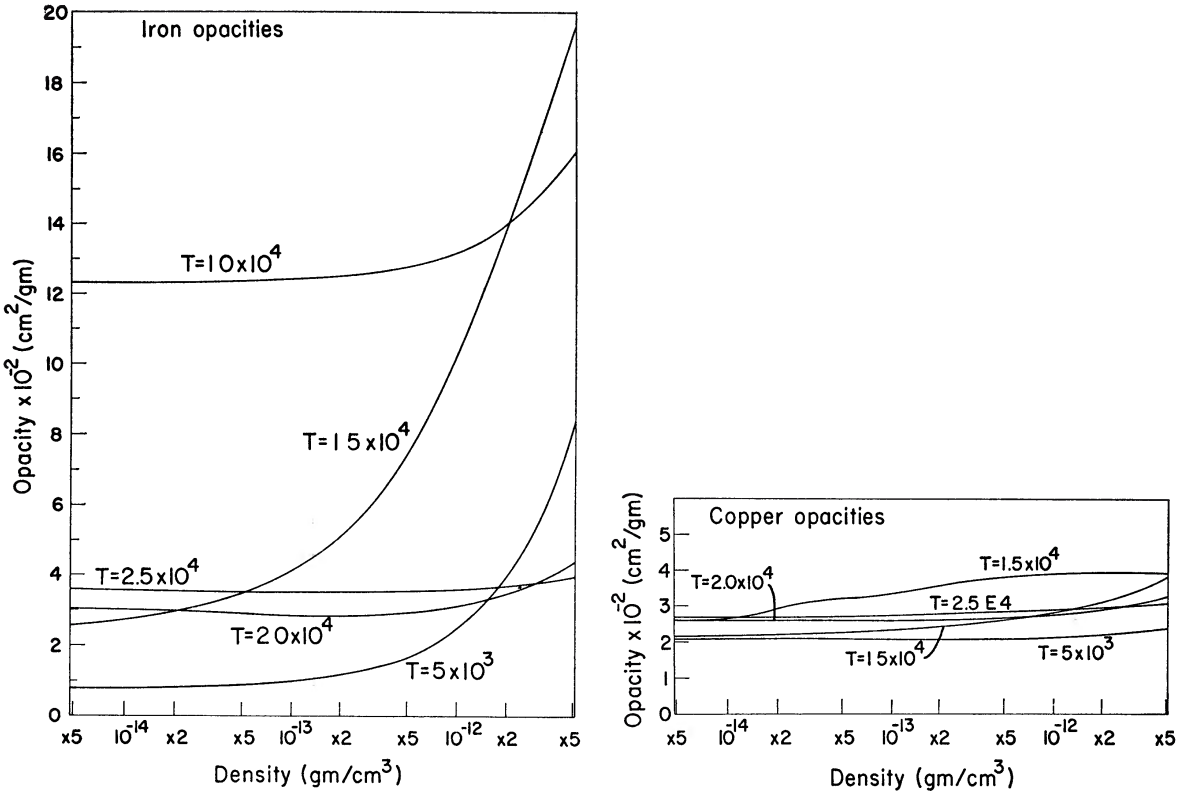

FIG 6 —Opacity of Fe as a function of temperature and density (Cox and Stewart 1965).
FIG. 7.—Opacity of Cu as a function of temperature and density (Cox and Stewart 1965).

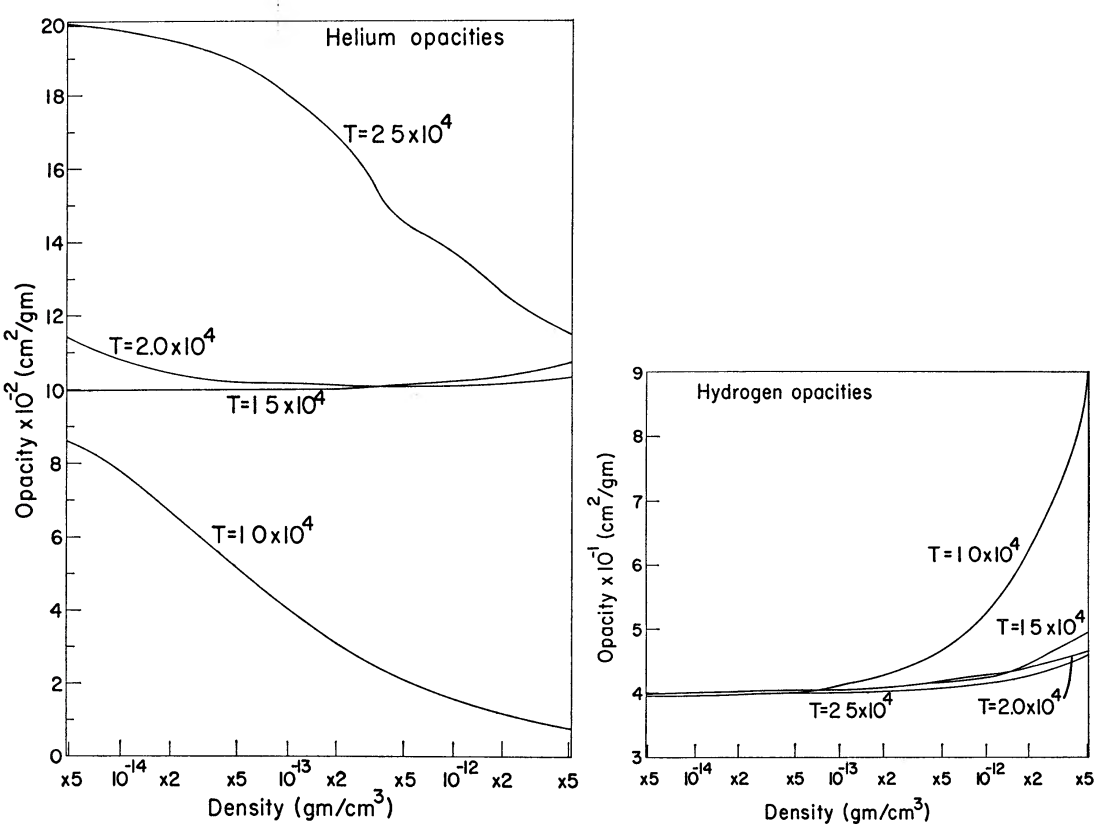

FIG. 8.—Opacity of He as a function of temperature and density (Cox and Stewart 1965).
FIG. 9.—Opacity of H as a function of temperature and density (Cox and Stewart 1965).

"shutter" behind. Numerical errors resulted in an oscillation and caused computational difficulty, but a small smoothing of the opacity law removed the instability—much as would be expected by the addition of light elements—and the result then becomes independent of the line contribution. In order for an instability to occur in the real case, a phase delay must be introduced as by hydrodynamics and an oscillation like that of a Cepheid variable will occur. The period becomes heat capacity/radiation = $3R/KcaT^3 \simeq 1$ sec.

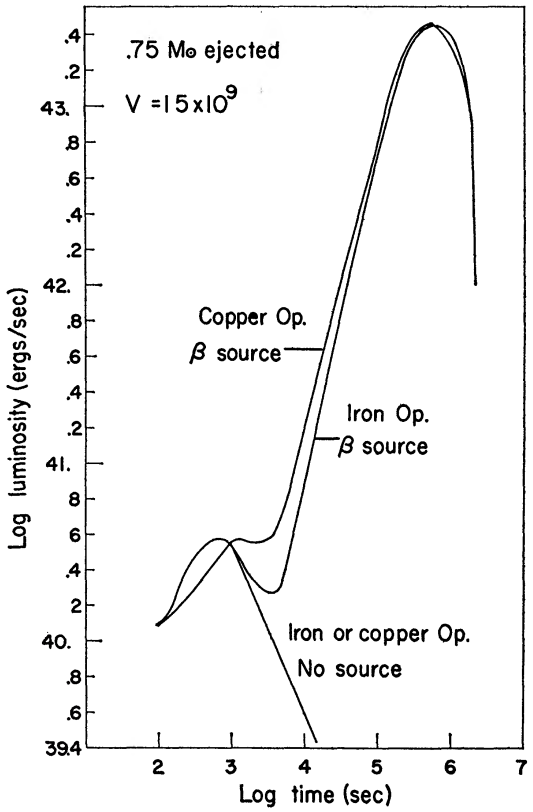

FIG. 10.—Log luminosity of 1.5 $M\odot$ supernova (0.75 $M\odot$ ejected) versus log time for both Fe and Cu opacity $V_1 = 1.5 \times 10^9$ cm sec^{-1}, $V_2 = 10^9$ cm sec^{-1}, and an erroneous source $S = S_1 e^{-\lambda_1 t} + 10 S_2 e^{-\lambda_2 t}$ (see eq. [23] in text). The similarity between the two curves indicates that the "line" contribution to the opacity is effectively "burned" out by the heat flux.

The main body of the results was therefore calculated by using the copper opacity ($\langle\mu\rangle = 37$) for the region emitting β-decay in order to simplify the computations. The external mantle of the 10 $M\odot$ supernova (7.25 $M\odot$) was assumed to be a mixture of 75 percent H and 25 percent He by number. The inner β-decay region of 0.75 $M\odot$ was the same as for the 1.5 $M\odot$ case. The justification for an "external mantle" is that in the collapse model of supernovae only the inner 1–2 $M\odot$ need be evolved to Si or Fe to result in collapse. The external matter will presumably be lighter in molecular weight. The assumption of the highest-opacity matter at these low densities is equivalent to the assumption of the lowest molecular weight, i.e., H and He. Even with this assumption of *highest*-opacity matter, the "mantle" is transparent at the time of luminosity maximum and hence does not affect the final light curve. The only effect of this matter is to partake in the velocity-distribution function (eqs. [1] and [3]). In this form, the equations of shock velocity and hence final velocity are not dependent on the initial

distribution of the mantle, so it applies equally well to an initial model of a red giant or a polytrope of index 3.

The results of the numerical calculations are shown in Figures 11–15 for the conditions given in Table 1.

Figures 11 and 12, the visual luminosity of several typical Type I supernovae (NGC 4621 and NGC 4636 [Minkowski 1964]) are indicated. The long time tail of the bolometric luminosity is indicated by a dashed curve normalized to the diffusion calculations at time t_0 for each curve. The calculation of this tail depends on the condition of γ-ray absorption transparency discussed in the next section. The diffusion calculation becomes invalid at time t_0 because the emissivity of the matter external to the surface is not—and, by the choice of boundary condition usual in diffusion theory, cannot be—included in the total emission. As a consequence, when the β-decay mass fraction external to the surface becomes a major fraction of the total β-decay matter (this fraction $\simeq$

TABLE 1

CONDITIONS FOR CALCULATIONS

FIGURE	EJECTED MASS, $M\odot$	OPACITY	t_0 (days)	$V_1\times10^{-9}$ (cm sec^{-1})	$V_2\times10^{-9}$ (cm sec^{-1})	INNER EJECTED MATTER		OUTER EJECTED MATTER $M\odot$(He+H)
						$M\odot$(^{56}Ni)	$M\odot$(^{28}Si)	
11, 12, 13	0 75	Cu	5 8	3	2	0 25	0 5	0
11, 12, 13	0 75	Cu	11	1 5	1	25	5	0
11, 12, 13	0 75	Cu	22	0 75	0 5	25	5	0
14, 15	8	Cu, H, He	22	3	2	25	5	7 25
14, 15	8	Cu, H, He	44	1 5	1	25	5	7 25
14, 15	8	Cu, H, He	88	0 75	0 5	0 25	0 5	7 25

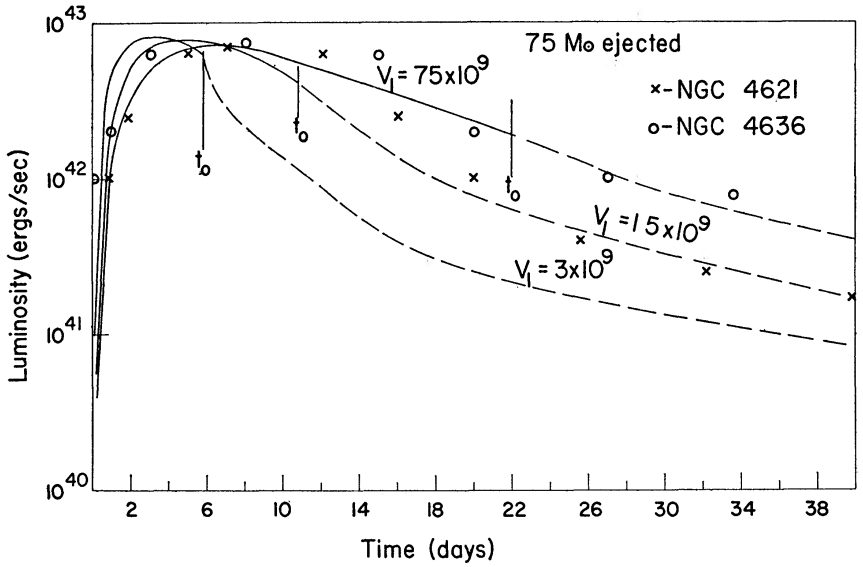

FIG. 11.—Log of luminosity versus time for the three velocity distributions of 0 75 $M\odot$ ejected from an initial 1 5 $M\odot$ star, V_1 = 0.75, 1.5, and 3 × 10^9 cm sec^{-1}; V_2 = 0.5, 1, and 2 × 10^9 cm sec^{-1}. The 0 75 $M\odot$ ejected mass was assumed to be 0.25 $M\odot$ ^{56}Ni and 0 5 $M\odot$ of ^{28}Si with an opacity corresponding to copper. Two observed Type II supernovae are included (*cross*, NGC 4621; *open circle*, NGC 4636); t_0 and the dashed curves are derived from the condition of γ-ray transparency.

$\frac{1}{2}$ at t_0), then the diffusion calculation loses validity and the transparency calculation of the following section becomes a better approximation. The bolometric correction to the theoretical curves is highly uncertain late in time because of near transparency. However, near maximum, where the temperature (Figs. 13 and 15) is about 6000°–7000°, the bolometric correction should be small. On the other hand, the observed colors of supernovae at this stage, as well as later, indicate a very much higher temperature of 10000°–30000° (Minkowski 1964; Zwicky 1965; Arp 1961). If the temperature were as high as 30000°, the total bolometric luminosity would have to be 30–60 times greater than calculated, and the β-decay energy source would be entirely inadequate. Instead, we propose that the temperatures are indeed as low as calculated and that the color is shifted toward the blue by the "fluorescence" of the very much larger projected area of the low-density, transparent, high-velocity material (see eq. [1]) external to the sur-

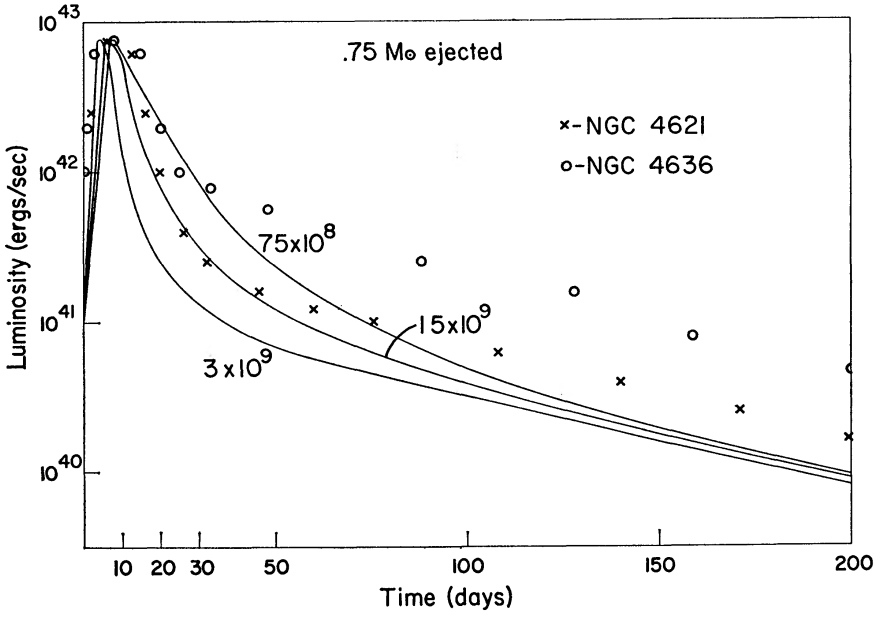

FIG. 12.—Log of luminosity versus time for the conditions of Fig. 12, but a longer time

face. After $t = t_0$, half the mass is transparent, and a typical 10 percent fluorescence of the γ recoil electron and/or β-decay would give almost 10 percent of the total emission in the blue-violet. This is enough to change the color temperature. With this interpretation, the bolometric magnitudes become the visual magnitudes. Within the relatively large error of this assumption, the Type II supernova, with an assumed larger mass 10 $M\odot$, makes qualitative sense, as is shown in Figures 14 and 15. The curves do not exhibit the usual "hump" associated with Type II supernovae—a sudden decrease at 20–40 days. Presumably, this could be added to the theory as fluorescence efficiency after transparency. In Figure 15, the two observed supernovae, NGC 7331 (Arp 1961) and NGC 5907 (Minkowski 1964) are normalized to the theoretical curve, $V_1 = 1.5 \times 10^9$ cm sec^{-1}, at the maximum. Actually, NGC 7331 was accurately measured photometrically, and the best estimate of the observed bolometric peak was at 1.2×10^{43} ergs sec^{-1}. The bolometric correction assumed for the observed value was small (0.5 mag), so the theoretical curves would require an increase by a factor of 1.4, or to 0.35 $M\odot$ of ^{56}Ni, to give agreement. The difference is within the error of the many assumptions involved in the model and calculations.

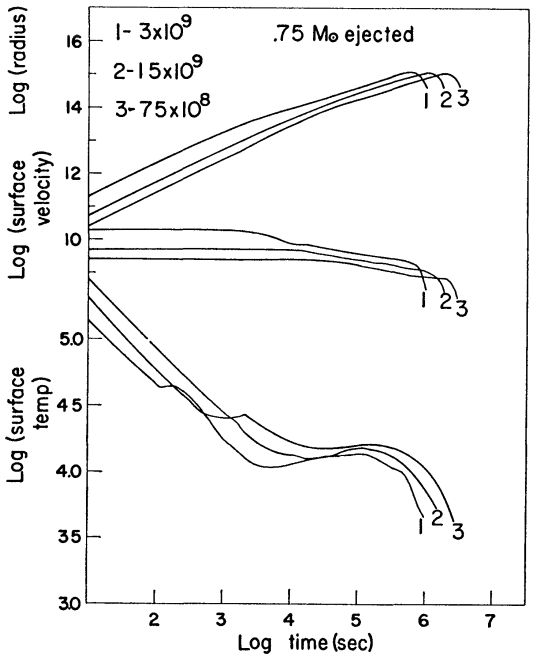

FIG. 13.—Surface temperature and surface velocity and radius versus time for the conditions of Fig. 12.

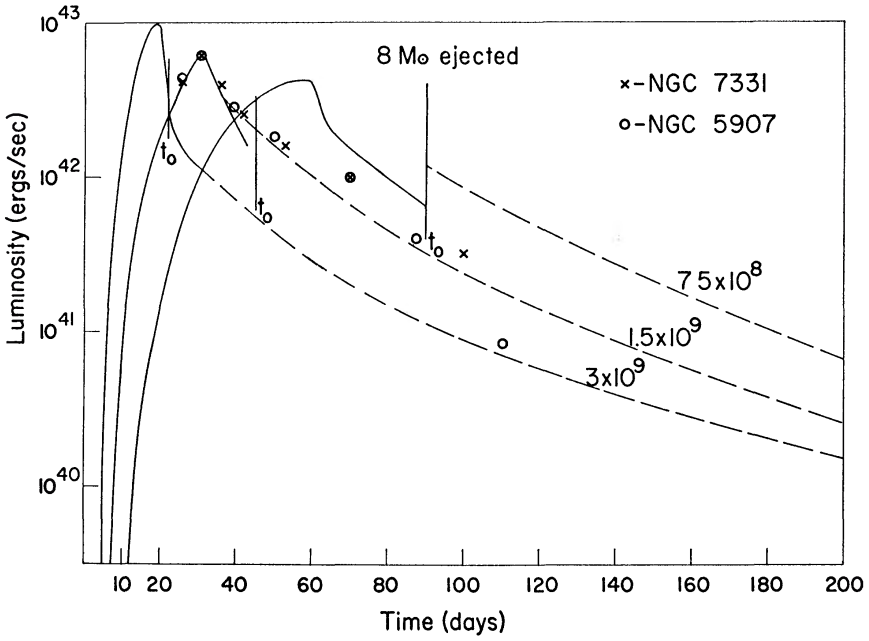

FIG 14.—Log luminosity versus time for the three velocity distributions of 8 $M\odot$ ejected from an initial 10 $M\odot$ star. $V_1 = 0.75$, 1.5, and 3×10^9 cm sec^{-1}; $V_2 = 0.5$, 1, and 2×10^9 cm sec^{-1}. The inner 0.75 $M\odot$ ejected mass was assumed to be 0.25 $M\odot$ ^{56}Ni and 0 5 $M\odot$ ^{28}Si with an opacity corresponding to that of copper. The outer ejected 7.25 $M\odot$ was assumed to be 75 percent H and 25 percent He by number with the corresponding opacity. Two observed Type I supernovae are included (*cross*, NGC 7331; *open circle* NGC 5907); t_0 and the dashed curves are derived from the condition of γ-ray transparency.

VII. LONGER-TIME LUMINOSITY

Finzi (1965) has advanced the idea that the long-time light curve depends on the decay of the residual vibrational energy of the neutron star. This excludes the possibility of thermonuclear supernovae. Burbidge *et al.* (1957) suggest the energy source ^{254}Cf, but the variability of the observed decay constant and the large mass of transuranic elements required casts some doubt on this mechanism. Morrison and Sartori (1966) have advanced the idea that the long-time decay of the optical luminosity is due to the fluorescence of helium in the interstellar medium excited by photons with energies of approximately 51 eV in the far-ultraviolet. The difficulty lies in the very large bolometric luminosity required to give the flux of ultraviolet photons. The energy

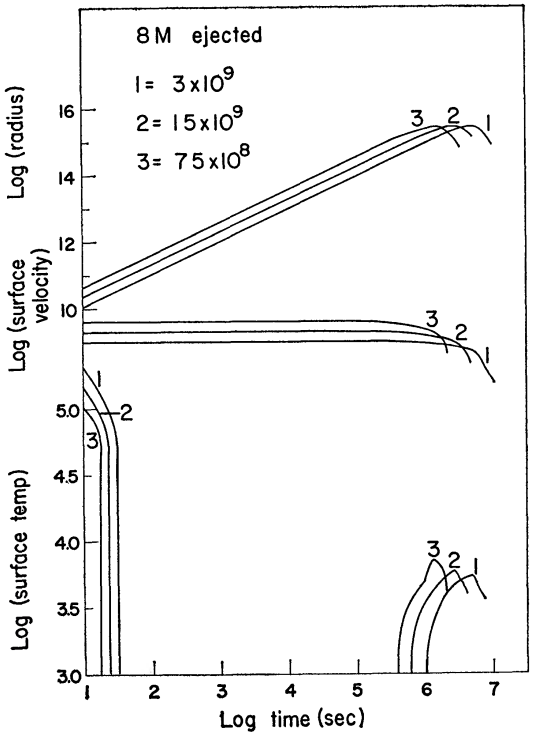

FIG. 15—Surface temperature, surface velocity, and surface radius versus time for the conditions of Fig. 14.

emitted in the slow-decay component (50–100 days) is variously 5×10^{48}–10^{49} ergs. The energy necessary to excite the necessary helium flourescence, under the assumption of the optimum interstellar density of helium, is a minimum of 5×10^{50}–10^{51} ergs of radiant energy.

At no period of the process of diffusive release could this energy be emitted without vastly changing the presumed physics of the whole phenomenon. Instead, we would rather associate the long-period luminosity decay as resulting from the 77-day β-decay of $^{56}Co \rightarrow {}^{56}Fe$. The changing efficiency for the self-absorption of the γ-ray fraction and the reduced efficiency for optical emission by line excitation and bremsstrahlung both conspire to result in a light curve that decays more rapidly that the basic 77-day period.

The mean γ-ray absorption coefficient for the ^{56}Co spectrum in the Si-Co-Fe mixture. is 0.04 cm^2 g^{-1}, so that 50 percent of the γ-ray energy escapes at a time when

$$\int_0^\infty \rho dr = 1/K \simeq 25 \text{ g cm}^{-2} . \quad (24)$$

At $T \simeq 10000°$, the optical opacity for copper (Ni + Si) is about the same as the γ-ray opacity, so that the optical transparency time t_0 is the same as the γ-ray transparency time. The subsequent fractional γ-ray deposition will decrease approximately as the thickness of the stellar matter $\langle \rho r \rangle \sim r^{-2} \sim (t/t_0)^{-2}$. This deposited energy first appears as recoil-electron kinetic energy, which, in turn, ionizes and excites atomic transitions. The effective recoil-electron, range, including multiple scattering in the Fe-Si mixture for a mean recoil energy of ~0.3–0.5 MeV, is approximately $\langle \lambda_{\text{recoil}} \rangle \sim 0.05$ g cm^{-2}. This corseponds to 500 times the γ-ray opacity, so the transparency condition for the recoil electrons is reached only at a time greater than 22 t_0, a time considerably longer than most observations. With the presence of many elements besides iron, the number of emission lines is so great that a major fraction of the excitation energy should appear in the optical spectrum. The lines will be broadened, owing to both Doppler spread and the very large self-absorption. The optical luminosity for $t_0 \leq t \leq 20\ t_0$ should then approximately follow the deposition of radioactive energy. In addition to the γ-ray emission from electron capture, $^{56}\text{Co} \rightarrow {}^{56}\text{Fe}$, there exists 20 percent β^+-emission (Fig. 1), where the positron has a mean kinetic energy of 0.75 MeV. The fractional energy, $f = (0.2 \times 0.75)/3.59 = 0.04$, deposited by these positrons (exclusive of the annihilation quanta) will not be subjected to the transparency attenuation as are the γ-rays. As a consequence, the late-time luminosity should be:

$$L = S_2 f + \left(\frac{t}{t_0}\right)^{-2} [S_1 + (1 - f) S_2]$$
$$= 0.015 \times 10^{43} e^{-\lambda_2 t} + \left(\frac{t}{t_0}\right)^{-2} (1.72 \times 10^{43} e^{-\lambda_1 t} + 0.362 \times 10^{43} e^{-\lambda_2 t}) \text{ ergs sec}^{-1}, \quad (25)$$

for 0.75 $M\odot$ ejected of one-third ^{56}Ni and two-thirds ^{28}Si.

In the case of the 1.5 $M\odot$ curves (Figs. 11 and 12), the luminosity is matched to the diffusion calculation at time t_0 by reducing the transparency luminosity by a factor of 0.7. This is a partial correction for the fraction of the β-decay matter external to the surface. For the 10 $M\odot$ curves (Fig. 14) no correction was made owing to the uncertainty in the model of the ^{56}Ni core and H-He shell.

VIII. DISCUSSION

The calculated light curves that best fit the observations are those for $V_1 \simeq 10^9$ cm sec^{-1}. The average kinetic energy is $\frac{1}{2} \langle V^2 \rangle = 0.41\ V^2_1$ for the velocity distributions used, so that the best fit for the case of the small supernovae is therefore 4.1×10^{17} ergs g^{-1}. On the other hand, the kinetic energy resulting from the complete thermonuclear burning of 1.42 $M\odot$ of ^{12}C (Hansen and Wheeler 1968) is 2.8×10^{17} ergs g^{-1}. One-half the fusion energy released is balanced by the initial net binding energy of the presupernova star. Other models may have substantially less binding energy. Finally, the theoretical kinetic energy should be increased because of the larger ejected mass (1.42 $M\odot$) compared with that of the calculated model, 0.75 $M\odot$. From equation (6), if t is kept constant (constant width of the light curve), then $V_1 = 2 \times 10^9$ cm sec^{-1} if the mass ejected is 1.5 $M\odot$. Then $\frac{1}{2} \langle V^2 \rangle = 1.6 \times 10^{18}$ ergs g^{-1}. This is 6 times larger than that predicted from thermonuclear energy alone for the Hansen model and 3 times larger than the absolute upper limit of thermonuclear energy. Roughly the same discrepancy in energy applies to the 10 $M\odot$ supernova because of the large inert envelope. The observed velocity of supernova envelopes ranges from 10^8 cm sec^{-1} for the older remnants with ages of 10^4 years (Poveda and Woltjer 1968), to the maximum velocity of 2×10^9 cm sec^{-1} observed for the most recent supernova in our Galaxy, Tycho's star, reported by Minkowski (1968).

At a late stage of expansion the light emission from the transparent remnant gases depends upon the second or higher power of the electron density, so it necessarily strongly

emphasizes the mass fractions of the slower-moving interior. The range of observed velocities is of the order of what would be expected, and the maximum observed velocity of 2×10^9 cm sec^{-1} qualitatively agrees with the mass average velocity $\langle V \rangle = 0.82$ $V_1 = 1.6 \times 10^9$ cm sec^{-1} for the ejected mass of 1.5 $M_\odot$.

Although no absolute conclusions can be made, the qualitative agreement between observed and predicted light curves substantiates the concept of the radioactive source of the luminosity and at least is consistent with both the thermonuclear and neutron-star origins of supernovae. To the best of the authors' present knowledge, no cobalt has been recognized in supernova spectra.

We are deeply indebted to Richard White for first writing the diffusion hydrodynamic program. The suggestion of James Truran concerning the importance of ^{56}Ni was the key to the problem. The opacity calculations of Arthur Cox and John Stewart of the Los Alamos Scientific Laboratory added greatly to the significance of the results. Professor Rudolph Minkowski has supplied many of the experimental curves, and Henry Lazarus has aided in the computations. This work was supported by the Astronomy Section, National Science Foundation, NSF grant GP-6810. W. D. Arnett has greatly contributed to the readability.

APPENDIX

The difference equations for the hydrodynamic part of the program have been given by Colgate and White (1966); therefore, we give only the difference equations for the section concerning diffusion. White's method is similar to that of Cox, Brownlee, and Eilers (1966) in that a system of n linearly coupled equations is used to solve for the temperatures at $n + 1$; however, differences exist in the methods of evaluating the radiation boundary condition, the diffusion coefficient, and the method of coupling the hydrodynamics to the radiation flow.

The equation to be solved is

$$\rho\epsilon_T \frac{\partial T}{\partial t} - \frac{1}{R^2}\frac{\partial}{\partial R}\left(R^2 D \frac{\partial T}{\partial R}\right) = 0\,, \tag{A1}$$

where T is the temperature, ϵ is the internal energy per unit mass, $\epsilon_T = (\partial\epsilon/\partial T)_\rho$, and ρ is the density.

Using the notation of Colgate and White, we difference equation (A1) in the following manner:

$$(\rho\epsilon_T R^2 \Delta R)^{n+0.5}_{j-0.5} \frac{T^{n+1}_{j-0\,5} - T^{n}_{j-0.5}}{\Delta t^{n+0.5}} - \left[\left(\frac{R^2 D}{\Delta R}\right)^{n+0.5}_{j}(T^{n+0.5}_{j+0\,5} - T^{n+0.5}_{j-0\,5}) - \left(\frac{R^2 D}{\Delta R}\right)^{n+0.5}_{j-1\,0}(T^{n+0.5}_{j-0.5} - T^{n+0.5}_{j-1\,5})\right] = 0\,, \tag{A2}$$

where the superscripts denote time and the subscripts denote zone numbers. We define

$$a^{n+0\,5}_{j} = 0.5\left(\frac{R^2 D}{\Delta R}\right)^{n+0.5}_{j} \Delta t^{n+0.5} \tag{A3}$$

and

$$b^{n+0.5}_{j-0.5} = (\rho\epsilon_T R^2 \Delta R)^{n+0.5}_{j-0\,5}\,. \tag{A4}$$

When equations (A3) and (A4) are substituted into equation (A2), we obtain

$$b^{n+0.5}_{j-0\,5}(T^{n+1.0}_{j-0\,5} - T^{n}_{j-0\,5}) - 2a^{n+0\,5}_{j}(T^{n+0.5}_{j+0.5} - T^{n+0.5}_{j-0\,5}) + 2a^{n+0\,5}_{j-1}(T^{n+0.5}_{j-0\,5} - T^{n+0.5}_{j-1\,5}) = 0\,. \tag{A5}$$

Letting

$$T^{n+0.5}_{j-0\,5} = 0.5(T^{n+1}_{j-0.5} - T^{n}_{j-0.5})$$

and substituting into equation (A5) yield

$$-a^{n+0.5}_{j-1\,0}T^{n+1.0}_{j-1.5} + (b^{n+0.5}_{j-0.5} + a^{n+0.5}_{j-1.0} + a^{n+0.5}_{j})T^{n+1\,0}_{j-0.5} - a^{n+0.5}_{j}T^{n+1.0}_{j+0\,5} = C_{j-0\,5}\,; \quad \text{(A6)}$$

$$-a^{n+0.5}_{j-1\,0}(T^{n}_{j-0.5} - T^{n}_{j-1.5}) + a^{n+0\,5}_{j}(T^{n}_{j+0.5} - T^{n}_{j-0\,5}) + b^{n+0.5}_{j-0.5}T^{n}_{j-0\,5} = C_{j-0\,5}\,. \quad \text{(A7)}$$

Equation (A6) is a set of linear simultaneous equations linear in T^{n+1} and can be solved by Gaussian elimination, if one uses the following relations in equations (A3) and (A4)

$$(R^{n+0\,5}_{j})^2 = \tfrac{1}{3}[(R^{n}_{j})^2 + R^{n}_{j}R^{n+1}_{j} + (R^{n+1}_{j})^2]\,; \quad \text{(A8)}$$

$$(R^2\Delta R)^{n+0.5}_{j-0.5} = \frac{\Delta m_{j-0.5}}{4\pi\rho^{n+0.5}_{j-0.5}}\,; \quad \text{(A9)}$$

$$\Delta R^{n+0\,5}_{j} = 0.5(\Delta R^{n+0.5}_{j+0.5} + \Delta R^{n+0.5}_{j-0\,5})\,; \quad \text{(A10)}$$

$$D^{n+0\,5}_{j} = \left(\frac{4ac}{3}\frac{T^3}{K\rho}\right)^{n+0\,5}_{j} = \frac{ac}{3}(T^{*n+0.5}_{j-0\,5} + T^{*n+0.5}_{j+0.5})[(T^{*n+0.5}_{j-0\,5})^2 + (T^{*n+0.5}_{j+0\,5})^2] \times \frac{\Delta R^{n+0.5}_{j+0.5} + \Delta R^{n+0.5}_{j-0.5}}{K^{n+0.5}_{j+}(\rho\Delta R)^{n+0\,5}_{j+0.5} + K^{n+0.5}_{j-}(\rho\Delta R)^{n+0\,5}_{j-0.5}}\,, \quad \text{(A11)}$$

where

$$T^{*n+0.5}_{j+0.5} = T^{n}_{j+0.5} + 1/2\,\frac{\Delta t^{n+0\,5}}{\Delta t^{n-0\,5}}(T^{n}_{j+0\,5} - T^{n-1}_{j+0.5})\,, \quad \text{(A12)}$$

$$K^{n+0.5}_{j+} = K(\langle T\rangle^{n+0\,5}_{j}, \rho^{n+0.5}_{j+0\,5})\,, \qquad K^{n+0.5}_{j-} = K(\langle T\rangle^{n+0.5}_{j}, \rho^{n+0.5}_{j-0.5})\,, \quad \text{(A13)}$$

$$\langle T\rangle^{n+0\,5}_{j} = 0.5(T^{*n+0.5}_{j+0.5} + T^{*n+0.5}_{j-0\,5})\,, \quad \text{(A14)}$$

and

$$4(T^{n+0.5}_{j})^3 = \left(\frac{T^4_{j+0.5} - T^4_{j-0.5}}{T_{j+0.5} - T_{j-0.5}}\right)^{n+0.5}\,. \quad \text{(A15)}$$

We therefore average neither the opacity nor the mean free path but rather the optical depth since it is this quantity which determines the absorption.

BOUNDARY CONDITIONS

To solve equation (A1), we furnish

$$T^{n+1}_{J+0\,5}$$

by imposing the Milne condition on the outer boundary. This approximation treats the star as a blackbody radiating into space from a surface two-thirds of a mean free path in from the actual surface with an effective temperature given by

$$T^4_{\text{effective}} = 2T^4_{\text{surface}}\,. \quad \text{(A16)}$$

If we consider the outermost zone whose boundaries are R_J and R_{J-1}, then the effective temperature can be determined by linear interpolation

$$\frac{T^4_e - T^4_s}{2\lambda/3} = \frac{T^4_{j-0.5} - T^4_s}{\frac{1}{2}\Delta R_{J-0.5}}\,, \quad \text{(A17)}$$

where λ is the mean free path. The use of equation (A16) in equation (A17) yields

$$T_e^4 = \frac{(8\lambda/3\Delta R_{J-0.5})T_{J-0.5}^4}{1 + 4\lambda/3\Delta R_{J-0\,5}} . \tag{A18}$$

Therefore, the flux F which crosses the outermost zone boundary J is

$$F = \frac{ac}{4} T_e^4 = \frac{(2ac\lambda/3\Delta R_{J-0.5})T_{J-0.5}^4}{1 + 4\lambda/3\Delta R_{J-0.5}} , \tag{A19}$$

whereas the flux computed by the difference equation is

$$F = -D_J \left(\frac{T_{J+0\,5} - T_{J-0.5}}{0.5\Delta R_{J-0\,5}} \right) . \tag{A20}$$

Equating equations (A19) and (A20), we find

$$D_J^{n+0\,5} = \frac{\frac{1}{3}ac(T^{*n+0.5}_{J-0.5})^3}{(K\rho\Delta R)^{n+0.5}_{J-0.5} + \frac{4}{3}} \Delta R_{J-0.5} , \tag{A21}$$

where we have set

$$T^{n+1}_{J+0.5} = 0 , \quad 1/\lambda = (K\rho)^{n+0.5}_{J-0.5} \tag{A22}$$

and

$$K^{n+0.5}_{J-0.5} = K(T^{*n+0.5}_{J-0\,5}, \rho^{n+0.5}_{J-0.5}) . \tag{A23}$$

For the inner boundary, we chose

$$T^{n+1}_{+0.5} = 0 , \quad D^{n+0.5}_{+1.0} = 0 , \tag{A24}$$

which is the condition of zero flux.

COUPLING OF HYDRODYNAMICS TO DIFFUSION

The equations for advancing temperature of Colgate and White (1966) allows one to compute

$$(\delta T^{n+0.5}_{j-0.5})_{\text{Hydro}} = T^{n+1}_{j-0.5} - T^n_{j-0.5} \tag{A25}$$

due to hydrodynamics above. Using one-half this increment, we advance the temperature,

$$\langle T \rangle = T^n + 0.5\delta T_{\text{Hydro}} , \tag{A26}$$

to obtain a mean temperature increase due to hydrodynamics alone. Then, if O defines the operation of the diffusion equation upon this mean temperature, the new temperature for the time step Δt^{n+1} is

$$T^{n+1} = O(T^n + 0.5\delta T_{\text{Hydro}}) + 0.5\delta T_{\text{Hydro}} . \tag{A27}$$

This procedure allows second-order accuracy if the operator is applied only to the temperatures which occur explicitly in equation (A7), but the diffusion coefficient and ϵ_T are assigned their mean extrapolated values from n to $n + 1$.

TIME STEPS

These controls are the same as those of Colgate and White with the exception that the energy is inhibited from changing more that 0.4 percent per cycle in any given zone.

SURFACE TEMPERATURE, RADIUS, VELOCITY, AND LUMINOSITY

To evaluate these surface quantities, we evaluate

$$\int_r^\infty K\rho dr = \tfrac{2}{3} \tag{A28}$$

to the nearest zone boundary denoted by j^*.

We then have

$$\text{Surface radius} = R_{j^*}^{n+0.5}; \quad \text{Surface velocity} = U_{j^*}^{n+0.5}; \tag{A29}$$

$$\text{Surface temperature} = \left[-\frac{4D_{j^*}^{n+0.5}}{ac}\left(\frac{T_{j^*+0.5}^{n+0.5} - T_{j^*-0.5}^{n+0.5}}{\Delta R_{j^*}^{n+0\,5}}\right)\right]^{0\,25} \tag{A30}$$

and

$$\text{Luminosity} = 4\pi(R_{j^*}^{n+0\,5})^2 \frac{ac}{4} \times (\text{surface temperature})^4 . \tag{A31}$$

REFERENCES

Arnett, W. D. 1967, *Canadian J. Phys.*, **44**, 2553.
———. 1968*a*, *Nature*, **219**, 1344.
———. 1968*b*, *Ap. J.*, **153**, 341.
Arp, H. C. 1961, *Ap. J.*, **133**, 883.
Bodansky, D., Clayton, D. D., and Fowler, W. A. 1968*a*, *Phys. Rev. Letters*, **20**, 161.
———. 1968*b*, *Ap. J. Suppl.*, **16**, 299.
Burbidge, E. M., Burbidge, G. R., Fowler, W. A., and Hoyle, F. 1957, *Rev. Mod. Phys.*, **29**, 547.
Cameron, A. G. W., and Arnett, W. D. 1967, *A.J.*, **72**, 292.
Clayton, D. D., Colgate, S. A., and Fishman, G. J. 1969, *Ap. J.*, **155**, 75.
Colgate, S. A. 1967, *Ap. J.*, **150**, 163.
———. 1968, in *Conf. Seyfert Galaxies and Related Objects* (Tucson, Arizona, February 1968 (to be published).
Colgate, S. A., and Cameron, A. G. W. 1963, *Nature*, **200**, 870.
Colgate, S. A., and White, R. H. 1966, *Ap. J.*, **143**, 626.
Cox, A. N., Brownlee, R., and Eilers, D. 1966, *Ap. J.*, **144**, 1024.
Cox, A. N., and Stewart, J. N. 1965, *Ap. J., Suppl.*, **11**, 22.
Erdelyi, A., Magnus, W., Oberhettinger, F., Tricomi, F. G. 1954, *Tables of Integral Transforms*, Vol. 1 (New York: McGraw-Hill Book Co.).
Finzi, A. 1965, *Phys. Rev. Letters*, **15**, 599.
Fowler, W. A., and Hoyle, F. 1964, *Ap. J. Suppl.*, **9**, 201 (No. 91).
Fraley, G. S. 1968, *Ap. and Space Sci.*, **2**, 96.
Hansen, C. J., and Wheeler, J. C. 1968, *Ap. and Space Sci.* (in press).
Hofmeister, E., Kippenhahn, R., and Weigert, A. 1964, *Zs. f. Astr.*, **60**, 57.
Jahnke, E., Emde, F., and Losch, F. 1960, *Tables of Higher Functions* (New York: McGraw-Hill Book Co.).
Lederer, C. M., Hollander, J. M., and Perlman, I. 1967, *Table of Isotopes* (6th ed.; New York: John Wiley & Sons).
Minkowski, R. L. 1964, *Ann. Rev. Astr. and Ap.*, **2**, 247.
———. 1968, in *Stars and Stellar Systems*, Vol. **7**, eds. B. M. Middlehurst and L. H. Aller, chap. 11 (Chicago: University of Chicago Press).
Morgan, A. J. A. 1952, *Quart. J. Math.* (Oxford), **2**, 250.
Morrison, P., and Sartori, L. 1966, *Phys. Rev. Letters*, **16**, 414.
Poveda, A. 1964, *Ann. d'ap.*, **27**, 522.
Poveda, A., and Woltjer, L. 1968, *A.J*, **73**, 65.
Rakavy, G., and Shaviv, G. 1967, *Ap. J.*, **148**, 803.
Schatzman, E. 1965, in *Stars and Stellar Systems*, Vol. **8**, eds. L. H. Aller and D. B. McLaughlin (Chicago: University of Chicago Press), p. 327.
Schwartz, R. A. 1967, *Ann. Phys.*, **43**, 42.
Truran, J. W. 1967, paper presented at Supernova Conference GISS, New York, November 1967.
Truran, J. W., Arnett, W. D., and Cameron, A. G. W. 1967, *Canadian J. Phys.*, **45**, 2315.
Truran, J. W., Cameron, A. G. W., and Gilbert, A. 1966, *Canadian J. Phys.*, **44**, 563.
Zwicky, F. 1965, in *Stars and Stellar Systems*, Vol. **8**, eds. L. H. Aller and D. B. McLaughlin (Chicago: University of Chicago Press), p. 397.